ISSN 0016-7029, Geochemistry International, 2006, Vol. 44, No. 6, pp. 581–590. © Pleiades Publishing, Inc., 2006.
Original Russian Text © S.V. Sokolov, S.A. Yarmishko, N.I. Chistyakova, 2006, published in Geokhimiya, 2006, No. 6, pp. 633–642.

Inclusions in Chrysolite from the Kovdor Massif: Genetic and Gemmological Significance

S. V. Sokolov[a], S. A. Yarmishko[b], and N. I. Chistyakova[a]

[a]*Fedorovskii All-Russia Institute of Mineral Resources (VIMS), Staromonetnyi per. 31, Moscow, 109017 Russia*
e-mail: vims-sokol@df.ru

[b]*Moscow State Geological Prospecting University, ul. Micklukho-Maklaya 23, Moscow, 117873 Russia*
e-mail: yarmishko@mtu-net.ru

Received October 14, 2004

Abstract—Gem-quality chrysolite (peridot) from a phlogopite deposit related to the Kovdor ultrabasic–alkaline massif in the Kola Peninsula, Russia, was studied using a variety of techniques (optical mineralogical microscopy, chemical, Mössbauer spectroscopy, and photoluminescence) to determine its chemical composition, the Fe^{2+}/Fe^{3+} ratio, refraction indexes, density, as well as to examine inclusions in it. Much attention was devoted to the microprobe identification of crystalline inclusions in the host chrysolite (apatite, tetraferriphlogopite, amphibole, and magnetite), its exsolution products (diopside and magnetite), and the daughter phases of melt inclusions in this mineral (which were subdivided into primary and secondary genetic types). The daughter phases of these melt inclusions are silicates (forsterite, diopside, tetraferriphlogopite, clinohumite, and serpentine), various carbonates (Ca-dominated carbonates are characteristic of the primary inclusions, whereas Mg-rich carbonates were found only in the secondary inclusions), magnetite, djerfisherite (alkali sulfide), and Ba–Sr–REE carbonates. The presence of melt inclusions testifies to a magmatic genesis of the gem, and the simultaneous occurrence of these inclusions with crystalline inclusions can be used as an additional identification feature of gem chrysolite from the Kovdor Massif.

DOI: 10.1134/S0016702906060048

INTRODUCTION

Chrysolite (peridot), a mineral of the olivine group, is a highly transparent gemstone of fine yellow or olive-green color. Chrysolite occurs at endogenous deposits of different genetic types [1] and is believed to be formed by means of crystallization from Mg-rich ultrabasic and basaltic melts or by the metasomatic transformation of dunites and peridotites. For example, chrysolite in alkaline–ultrabasite and carbonatite massifs was thought to be of metasomatic genesis.

The study of internal micromineralogy of gemstones (inclusions of crystalline phases that crystallized before and/or simultaneously with their host mineral), exsolution products, and melt and fluid inclusions of the mineral-forming medium provides gemmological and genetic information that is of applied and scientific importance: (1) it serves as an identification feature of gemstones; (2) makes it possible to pinpoint the deposit from which the mineral originates or to identify the primary sources of stone material collected in placers; (3) sometimes allows an expert to distinguish between natural and synthetic minerals; and (4) provides clues to the geneses of natural gemstones.

Chrysolite from deposits of different types contains inclusions differing in mineral and chemical composition, morphologic features, and the character of their distribution in the host mineral crystal [1, 2]. For example, kimberlitic chrysolite from various deposits typically bears inclusions of enstatite, Cr-diopside, pyrope, and chromite. Chrysolite from Hawaii contains rounded glass inclusions with Cr-spinel crystals on the surface. A distinctive feature of samples from the San Carlos deposit, United States, is the presence of unusual so-called lily-pad inclusions, which are Cr-spinel crystals surrounded by crescent cracks hosting tiny fluid inclusions. Chrysolite of the Zeberged deposit, which has been known since ancient times, contains multiphase crystal–fluid inclusions with halite as a daughter phase (which accounts for 30–50% by volume), aqueous solution, and a gas bubble [3].

In an earlier paper [4], we described crystalline and multiphase melt inclusions in chrysolite from ultrabasic–alkaline rocks and carbonatites, such as Kovdor in the Kola Peninsula and Kugda in Polar Siberia. This paper presents the results of our complex (petrographic, mineralogical, microprobe, and spectroscopic) research of these inclusions in chrysolite from rocks of the Kovdor phlogopite deposit.

GEOLOGICAL SETTING AND CHARACTERISTICS OF CHRYSOLITE

The Kovdor massif of ultrabasic, alkaline rocks, and carbonatites is located in the southwestern part of the Kola Peninsula and is hosted by gneisses and granite-

Table 1. Chemical composition (wt %) of chrysolite

Component	Min. and max. concentrations	Average (n = 12)
SiO_2	39.18–40.79	40.12
TiO_2	0.00–0.13	0.04
Al_2O_3	0.03–0.18	0.09
FeO_t	10.49–11.70	11.30
MnO	0.36–0.66	0.52
MgO	46.97–48.27	47.45
CaO	0.21–0.44	0.36
NiO	0.06–0.20	0.12
Na_2O	0.18–0.31	0.26
K_2O	n.d.	n.d.
Total	–	100.26
Fa, mol %	10.9–12.1	11.8

Note: n.d. means not detected.

gneisses of Archean age. The massif is a multiple intrusion with a zonal structure [5, 6], which was formed by successive injections of various silicate rocks (from olivinites to syenites), phoscorites, and carbonatites with a close association of magmatic metasomatic processes. The massif is accompanied by apatite–magnetite and phlogopite mineral deposits

Olivine, one of the main rock-forming minerals of the massif, is contained in variable amounts in the ultramafites (olivinites, peridotites, and olivine pyroxenites), olivine–monticellite rocks, olivine-bearing alkaline rocks (turjaites, melteigite porphyries), phoscorites, and calcite carbonatites. However, chrysolite, a gem variety of olivine, occurs only in rocks of the phlogopite complex.

The Kovdor phlogopite deposit is restricted to the contact zone between olivinites and melilitolites in the northwestern part of the Kovdor massif [6, 7]. The marginal part of the orebody is composed of fine-grained phlogopite–diopside–forsterite rocks, which grade to giant-grained varieties of the same composition toward the central part of the deposit. The orebody itself comprises several bodies of phlogopite–diopside–forsterite pegmatoid rocks. The core of the largest phlogopite body (the Main Phlogopite Orebody) consists of coarse-grained forsteritite with calcite pockets. The latter contain gem-quality chrysolite in association with apatite, tetraferriphlogopite, and magnetite.

Chrysolite occurs in the cores of euhedral prismatic olivine crystals, which occasionally reach 10–15 cm in length. The refraction indexes of chrysolite were determined on a refractometer to be as follows: n_g = 1.689–1.690, n_m = 1.669–1.672, n_p = 1.654–1.656, $n_g - n_p$ = 0.034–0.035. The density (determined by the volumetric method) ranges from 3.35 to 3.39 g/cm^3.

Chrysolite from the Kovdor Massif commonly bears inclusions of various minerals, exsolution phases, and multiphase recrystallized melt inclusions, on which our research was centered.

EXPERIMENTAL

The host chrysolite and all varieties of its inclusions were studied under a microscope in doubly polished platelets prepared of chrysolite grains. Phases were preliminarily identified under an optical microscope and then confirmed by microprobe analyses. The chemical compositions of chrysolite, its mineral inclusions, and the daughter phases of its melt inclusions were determined on Jeol 733 Superprobe and JXA-8100 Superprobe electron microprobes equipped with a Link INCA-400 X-ray energy dispersive spectrometer. The standards were natural minerals of known composition, metals, and synthetic compounds: diopside for Si, Mg, and Ca; rutile for Ti; microcline for Al and K; almandine for Fe; rhodonite for Mn; chkalovite for Na; pyrite for Fe and S; chalcopyrite for Cu; sphalerite for Zn; metals for Ni and Co; SrF_2 for Sr; BaF_2 for Ba; K_2ReCl_6 for Cl; GaP for P; LaF_3 for La; CeF_3 for Ce and F; PrF_3 for Pr; and NdF_3 for Nd. Some phases of melt inclusions (first of all, some carbonates) were thermally unstable under the electron beam (at an accelerating voltage of 20 kV and a beam current of 15–20 nA), and therefore, they were analyzed on an energy dispersive spectrometer, which made it possible to simultaneously determine all components at a single analytical spot at counting times of 50–100 s and a relatively low beam current of ~5 nA. Trace components with contents of less than 1 wt % were analyzed on a WDS by the crystal diffraction method.

In order to determine Fe^{2+} and Fe^{3+} in the chrysolite structure and to estimate the ferrous/ferric ratio, we used optical spectroscopy (absorption spectra were obtained on a Philips PU 8800 spectrophotometer) and by Mössbauer spectrometry on a YAGRS-4M spectrometer.

RESULTS AND DISCUSSION

The results of microprobe analysis (Table 1) show that the host chrysolite contains from 10.9 to 12.1 mol % of the fayalite end member and trace amounts of MnO (0.36–0.66%), NiO (up to 0.2%), and CaO (0.21–0.44%).

The absorption spectra include bands with maxima at ~385, 450, 485, and 615 nm, which are caused by the presence of Fe^{2+} and Fe^{3+}, which are the major chromophores and they determine the color of this gem [8]. Mössbauer spectroscopic data (NGR method, analyst V.V. Korovushkin, Fedorovskii All-Russia Institute of Mineral Resources) indicate that bivalent iron prevails in the chrysolite over trivalent iron (Fe^{2+}/Fe^{3+} = 10.64), a fact suggesting a relatively low oxygen fugacity during the crystallization of this mineral. This also follows

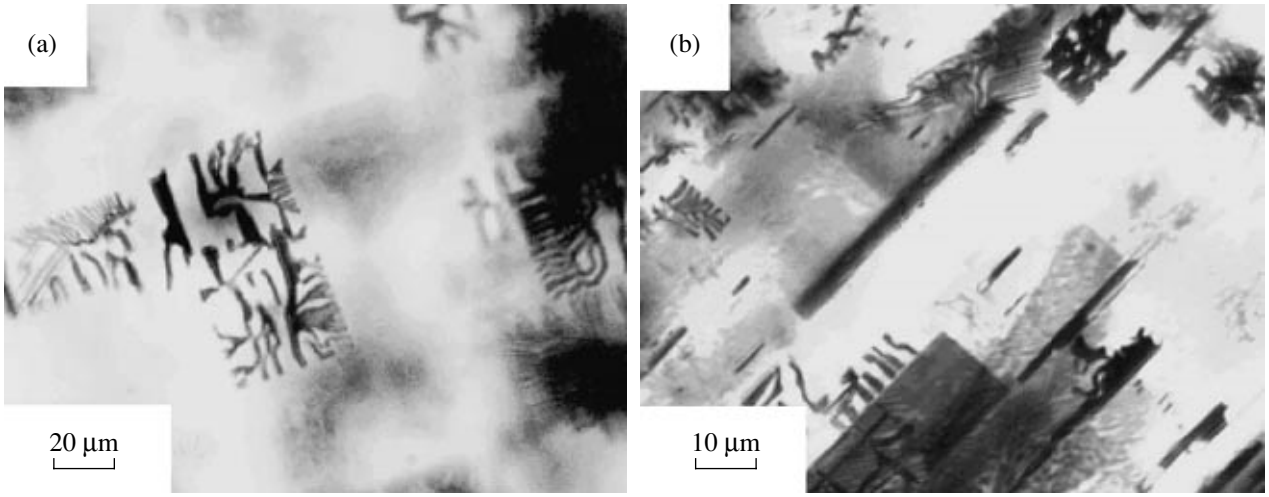

Fig. 1. Exsolution textures in chrysolite: (a) dendritic and (b) two-phase among dendritic inclusions (in the central part of the micrograph).

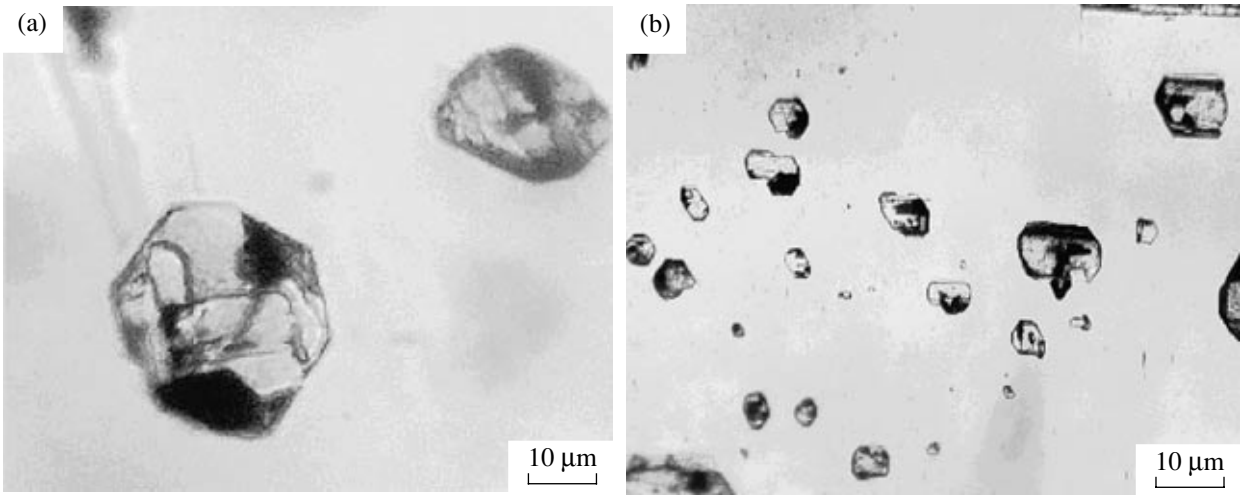

Fig. 2. Recrystallized inclusions in chrysolite: (a) primary, (b) secondary.

from the presence of hydrocarbons in melt and fluid inclusions in olivine and apatite from forsteritites of the Kovdor phlogopite deposit [9].

Our spectroscopic data explain the color of the Kovdor chrysolite and specific features of its scale of colors. It is known [10] that the presence of Fe^{2+} in olivine results in its green color, whose intensity increases with increasing the Fe^{2+} content, and the presence of even small amounts of Fe^{3+} in chrysolite brings about yellow tints.

Crystalline inclusions. The cores of chrysolite crystals contain inclusions of short-columnar crystals of early apatite-I, and the rim zones of the chrysolite crystals include long-prismatic crystals of late apatite-II. Both generations of apatite exhibit hexagonal cross-sections and straight extinction (Figs. 1, 2). Apatite-II is sometimes accompanied by acicular and flat-prismatic crystals of amphibole. Platelets of mica, which are evenly distributed in chrysolite, have perfect cleavage, a brownish-red color, strong pleochroism, and a reverse absorption scheme. These properties led us to classify this mica with tetraferriphlogopite. Magnetite ingrowths in tetraferriphlogopite are usually equant and often euhedral. The magnetite has rather high reflectivity in reflected light and a grayish-white color, sometimes with pinkish tints.

Apatite-I is characterized by low contents of Sr and REE and is high in F. Compared to it, apatite-II is enriched in Sr, La, and Ce, but bears virtually no F (Table 2). These apatite crystals contain, along with La and Ce, other LREE, whose concentrations are below the detection limit of the analyzers. It was definitely determined that this mineral contains Dy and Sm, whose bands are clearly seen in the photoluminescence spectra of the apatite. The spectra obtained by V.A. Ras-

Table 2. Chemical compositions (wt %) of (1–5) crystalline inclusions and (6, 7) exsolution products in chrysolite

Component	Mineral						
	Apatite-I (4)*	Apatite-II (2)	Amphibole (2)	Tetraferriphlogopite (3)	Magnetite (2)	Diopside (1)	Magnetite (1)
	@						
	1	2	3	4	5	6	7
SiO_2	–	–	58.42	40.94	–	53.62	–
TiO_2	–	–	0.18	n.d.	0.23	n.d.	0.14
Cr_2O_3	–	–	–	–	0.15	0.20	0.34
Al_2O_3	–	–	0.16	0.68	0.04	0.33	0.20
FeO_t	0.04	0.33	3.58	15.85	82.28	2.45	87.58
MnO	<0.04	0.05	0.22	0.08	0.56	0.07	0.14
MgO	0.05	n.d.	22.95	26.40	2.36	18.69	2.45
CaO	55.18	54.91	4.54	0.26	0.20	24.96	0.09
SrO	0.14	1.00	–	n.d.	–	–	–
BaO	–	–	–	0.10	–	–	–
NiO	–	–	–	–	0.31	0.02	0.14
Na_2O	0.05	0.24	8.28	0.32	–	0.44	–
K_2O	n.d.	n.d.	0.83	9.73	–	n.d.	–
La_2O_3	<0.06	0.14	–	–	–	–	–
Ce_2O_3	0.10	0.25	–	–	–	–	–
P_2O_5	40.46	40.80	–	0.11	–	–	–
F	0.56	traces	n.d.	n.d.	–	–	–
Cl	<0.05	n.d.	n.d.	n.d.	–	–	–
Total	96.49**	97.72	99.16	94.47	86.13	100.78	91.08

* Numerals in parentheses correspond to the numbers of analyses.
** Analytical total including –O=F 0.24%.
n.d. means not detected.

sulov (Fedorovskii All-Russia Institute of Mineral Resources) using an LGI-505 laser with $\lambda_{rad} = 337.1$ nm showed characteristic bands of Dy^{3+} (at 480 and 570 nm) and Sm^{3+} (at 560, 600, and 640 nm).

The amphibole that crystallized with apatite-II contains only trace amounts of F and can be classified as richterite according to its chemical composition. In contrast to the micas of the biotite-phlogopite series, the tetraferriphlogopite is deficient in Al, whose structural site is partly occupied by Fe^{3+} [11]. The magnetite is characterized by high Mg, Ni, and Cr contents (Table 2).

Exsolution textures. Olivine and forsterite from the Kovdor ultramafic, monticellite, and phlogopite rocks ubiquitously contain single-phase (magnetite) and two-phase (pyroxene and magnetite) inclusions, which are oriented along certain crystallographic direction of the host crystals and were produced by the exsolution of solid solutions [5, 12]. We were the first to find morphologicaly similar distectic products in chrysolite, which contains them in the cores of its crystals. Most of these inclusions, which are very unusual in chrysolite (found only in a single sample), look like black dendrites, although some of these inclusions have more complicated morphologies and consist of rectangular platelets and dendrites around them (Fig. 1a). Some inclusions are as large as 35–40 μm across and a few micrometers thick, which made it very difficult to prepare polished platelets for microprobe analysis with these minerals exposed at the surface. Because of this, we failed to quantitatively determine their composition, but qualitative data indicate that inclusions of this type are magnetite.

The dendrites are in places accompanied by two-phase flattened inclusions in which one phase (commonly larger) is black opaque and the other shows oblique extinction. These inclusions are parallel and are up to 10–12 μm long and 3–4 μm wide (Fig. 1b). The pale transparent phase of the inclusions is diopside, and their black phase is magnetite (Table 2).

The character of the distribution of these inclusions in chrysolite, its almost constant chemical composition, and the absence of secondary alterations provide good

Table 3. Chemical compositions (wt %) of the daughter phases of primary melt inclusions

Component	Daughter phase									
	forsterite (7)*	diopside (5)	tetraferriphlogopite (6)	clinohumite (1)	magnetite (5)	apatite (2)	calcite (4)	shortite (4)	nyerereite (1)	Na–Ca carbonate (2)
SiO_2	41.33	54.26	40.06	35.94	–	–	–	–	–	–
TiO_2	0.09	0.10	0.07	1.30	0.17	–	–	–	–	–
Cr_2O_3	–	–	–	0.10	0.09	–	–	–	–	–
Al_2O_3	0.07	0.15	0.10	0.06	0.13	–	–	–	–	–
FeO_t	4.78	2.07	18.55	4.93	90.17	0.08	0.66	0.51	0.63	0.59
MnO	0.67	0.05	0.11	0.48	0.42	0.04	0.07	0.03	0.07	0.05
MgO	52.09	18.10	24.78	55.27	1.13	0.07	0.29	0.27	0.25	0.28
CaO	0.29	25.49	0.21	0.18	0.38	56.04	53.70	35.46	25.50	39.94
SrO	–	–	0.14	–	–	0.75	0.48	–	–	0.10
BaO	–	–	0.18	–	–	0.19	0.16	–	–	0.05
NiO	0.08	0.11	0.06	n.d.	0.11	–	–	–	–	–
Na_2O	0.11	0.28	0.42	0.13	n.d.	0.18	0.24	18.41	30.89	12.88
K_2O	n.d.	0.06	9.40	n.d.	n.d.	n.d.	0.05	0.24	0.11	0.20
P_2O_5	–	–	–	–	–	41.48	–	–	–	–
La_2O_3	–	–	–	–	–	n.d.	n.d.	n.d.	n.d.	n.d.
Ce_2O_3	–	–	–	–	–	n.d.	n.d.	n.d.	n.d.	n.d.
F	–	–	n.d.	n.d.	–	n.d.	–	–	–	–
Cl	–	–	n.d.	n.d.	–	n.d.	–	–	–	–
CO_2**	–	–	–	–	–	–	43.32	41.64	42.70	41.32
Total	99.51	100.67	94.08	98.39	92.50	98.83	98.87	96.56	100.15	95.41

* Numerals in parentheses correspond to the numbers of analyses
** Calculated from stoichiometric considerations.
n.d. means not detected.

reasons [13] to suggest that the origin of the solid inclusions was not associated with the addition of material, but was caused by the redistribution of components during the exsolution of the solid solution. This process was initiated by the tendency toward the structural ordering of the chrysolite with temperature decreasing after the crystallization of this mineral. The released Fe and Mg were partly exsolved in the form of magnetite, and the excess Si and Ca (together with Mg) formed diopside.

Melt inclusions. The Kovdor chrysolite contains abundant melt inclusions, which are made up of a multiphase aggregates of daughter minerals. Microscopic study allowed us to classify them into two genetic types: (1) primary inclusions, which are portions of melt trapped during chrysolite crystallization (individual inclusions or groups of closely spaced inclusions randomly distributed in the volume of the host mineral) and (2) secondary inclusions, which are residual melts (they cluster in microfractures in chrysolite). All inclusions are equant or slightly elongated and usually subhedral, and the primary inclusions are often negative olivine crystals (Fig. 2). The sizes of the inclusions vary within a wide range; the primary inclusions are usually larger, most of them are 40–50 μm in diameter, and some of them are even as large as 80 μm. However secondary inclusions sometimes can be as large as 120 μm.

Our analytical data indicate that melt inclusion of both genetic types contains both analogous and different mineral phases (Tables 3–5 and Figs. 3, 4). The primary inclusions typically have little varying phase compositions and consist of magnesian silicates (forsterite, tetraferriphlogopite, clinohumite), magnetite, and Ca-bearing minerals [diopside, apatite, calcite, and Na–Ca carbonates, such as shortite $Na_2Ca_2(CO_3)_3$ and nyerereite $Na_2Ca(CO_3)_2$]. It should also be noted that the inclusions contain carbonates, which are likely solid solutions of the Na_2CO_3–$CaCO_3$ series. The possible occurrence of such phases in Ca–Na–K carbonate systems was confirmed experimentally [14].

The secondary inclusions differ from the primary ones by having very variable phase compositions, which were likely caused by the multicomponent com-

Table 4. Chemical compositions (wt %) of the daughter phases of secondary melt inclusions

Component	Daughter phase								
	forsterite (3)*	tetraferriphlogopite (4)	clinohumite (1)	serpentine (4)	magnetite (5)	apatite (1)	shortite (5)	K–Na–Ca carbonate (2)	Mg–Na–Ca carbonate (5)
SiO_2	39.70	40.64	37.32	41.64	–	–	–	–	–
TiO_2	0.11	0.02	0.41	n.d.	0.07	–	–	–	–
Al_2O_3	0.05	0.04	n.d.	0.03	0.08	–	–	–	–
FeO_t	7.44	18.48	4.43	3.78	89.11	n.d.	0.83	0.46	0.49
MnO	0.49	0.08	0.30	0.16	0.67	n.d.	0.08	0.04	0.06
MgO	51.74	26.28	54.77	41.72	0.90	n.d.	1.08	1.08	2.14
CaO	0.02	0.08	0.08	0.22	0.23	56.41	34.92	32.50	31.79
SrO	–	0.28	–	–	–	1.06	0.20	0.23	0.83
BaO	–	0.27	–	–	–	n.d.	0.20	0.06	0.27
NiO	0.03	–	–	0.03	0.06	–	–	–	–
Na_2O	0.52	0.23	0.47	0.54	–	–	17.42	19.18	20.73
K_2O	0.03	10.26	n.d.	0.06	–	–	0.17	2.54	0.10
La_2O_3	–	–	–	–	–	0.12	0.23	0.24	0.14
Ce_2O_3	–	–	–	–	–	0.28	0.30	0.30	0.08
Pr_2O_3	–	–	–	–	–	n.d.	0.31	n.d.	n.d.
Nd_2O_3	–	–	–	–	–	n.d.	n.d.	0.07	0.05
P_2O_5	–	–	–	–	–	41.64	–	–	0.11
F	–	n.d.	n.d.	–	–	n.d.	–	–	–
Cl	–	n.d.	n.d.	–	–	n.d.	–	–	–
CO_2**	–	–	–	–	–	–	42.06	42.02	42.92
Total	100.13	96.66	97.78	88.18	91.12	99.51	97.80	98.82	99.71

Component	Daughter phase									
	dolomite (2)	eitelite (6)	bradleyite (5)	northupite (4)	Na–Mg–Ba carbonate (2)	barytocalcite (2)	burbankite (7)	carbocernaite (?) (4)	djerfisherite (7)	
SiO_2	–	–	–	–	–	–	–	–	Fe	47.75
TiO_2	–	–	–	–	–	–	–	–	Mn	0.10
Al_2O_3	–	–	–	–	–	–	–	–	Mg	1.45
FeO_t	1.18	0.66	0.32	0.55	0.32	0.78	0.72	0.68	Ca	0.33
MnO	0.43	1.22	0.57	1.00	0.18	0.03	0.06	0.05	Sr	0.18
MgO	20.85	21.52	16.10	15.27	18.26	0.67	0.89	0.33	Ba	n.d.
CaO	29.95	0.69	0.11	0.70	0.98	18.18	13.73	11.69	Na	1.44
SrO	0.30	0.13	0.28	0.33	0.40	1.82	17.70	20.61	K	9.05
BaO	0.12	0.06	n.d.	0.12	33.15	46.84	13.37	14.82	Ni	2.89
NiO	–	–	–	–	–	–	–	–	Co	0.92
Na_2O	0.16	27.74	30.82	29.15	8.98	0.49	11.08	3.90	Zn	0.22
K_2O	0.03	0.04	0.06	0.18	0.18	0.02	0.48	0.11	Cu	0.03
La_2O_3	0.04	–	–	–	–	–	2.85	3.38	S	31.96
Ce_2O_3	0.21	–	–	–	–	–	3.60	4.07	Cl	1.42
Pr_2O_3	n.d.	–	–	–	–	–	0.18	0.16		
Nd_2O_3	n.d.	n.d.	–	–	–	–	0.32	0.64		
P_2O_5	–	n.d.	29.94	–	–	–	–	–		
F	–	n.d.	n.d.	n.d.	n.d.	–	–	–		
Cl	–	n.d.	n.d.	11.69	n.d.	–	–	–		
CO_2**	47.64	44.98	18.33	32.20	37.15	30.07	34.46	29.13		
Total	100.91	97.04	96.53	91.19	99.60	98.90	99.44	89.57		97.74

Notes: * Numerals in parentheses correspond to the numbers of analyses.
** Calculated from stoichiometric considerations.
n.d. means not detected.

Table 5. Differences between the phase and chemical compositions of the primary and secondary melt inclusions

Primary melt inclusions	Secondary melt inclusions
Forsterite (Fa 4.9 mol %)	Forsterite (Fa 7.4 mol %)
Diopside	–
Tetraferriphlogopite (Al_2O_3 0.10; SrO 0.14; BaO 0.18; K_2O 9.40)	Tetraferriphlogopite (Al_2O_3 0.04; SrO 0.28; BaO 0.27; K_2O 10.26)
Clinohumite (TiO_2 1.30)	Clinohumite (TiO_2 0.41)
–	Serpentine
Magnetite (TiO_2 0.17; Cr_2O_3 0.09; MgO 1.13; NiO 0.11)	Magnetite (TiO_2 0.07; Cr_2O_3 0.00; MgO 0.90; NiO 0.06)
Apatite (REE_{Ce} 0.00; SrO 0.75)	Apatite (La_2O_3 0.12; Ce_2O_3 0.28; SrO 1.09)
Calcite (MgO 0.29)	–
Shortite (MgO 0.27; REE_{Ce} 0.00)	Shortite (MgO 1.08; REE_{Ce} 0.84)
Nyerereite (MgO 0.25)	–
Na-Ca carbonate (MgO 0.28)	Na–Ca carbonate (MgO 2.14)
–	K–Na–Ca carbonate (MgO 1.08)
–	Dolomite
–	Eitelite
–	Bradleyite
–	Northupite
–	Barytocalcite
–	Burbankite
–	Carbocernaite (?)
–	Djerfisherite

Note: Concentrations are given in wt %.

positions of the residual melts enriched in incompatible elements. In addition to diopside, clinohumite, calcite, and nyerereite, they contain the same phases as those of the primary inclusions and additionally bear widespread serpentine, dolomite, and Na–Mg carbonates: eitelite $Na_2Mg(CO_3)_2$, bradleyite $Na_3Mg(CO_3)(PO_4)$, and northupite $Na_3Mg(CO_3)_2Cl$. The secondary inclusions additionally contain djerfisherite, a rare alkaline sulfide $K_6Na(Fe, Ni, Cu)_{24}S_{26}Cl$, and carbonates rich in Ba, Sr, and REE: barytocalcite $BaCa(CO_3)_2$,

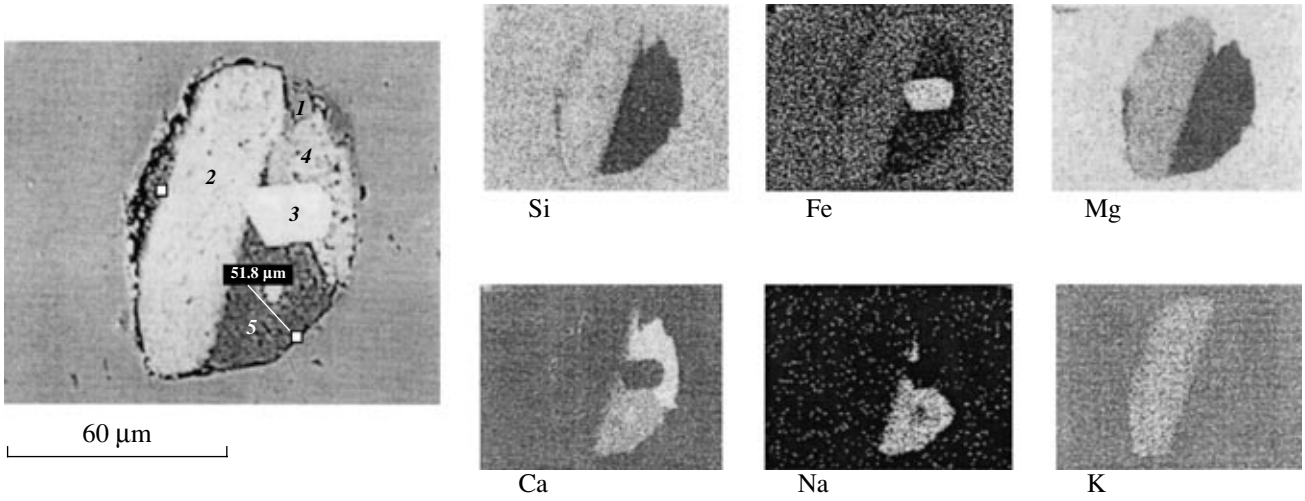

Fig. 3. Back-scattered and characteristic X-ray radiation images of a primary magmatic inclusion and its daughter phases: (*1*) forsterite, (*2*) tetraferriphlogopite; (*3*) magnetite, (*4*) calcite, (*5*) Na–Ca carbonate.

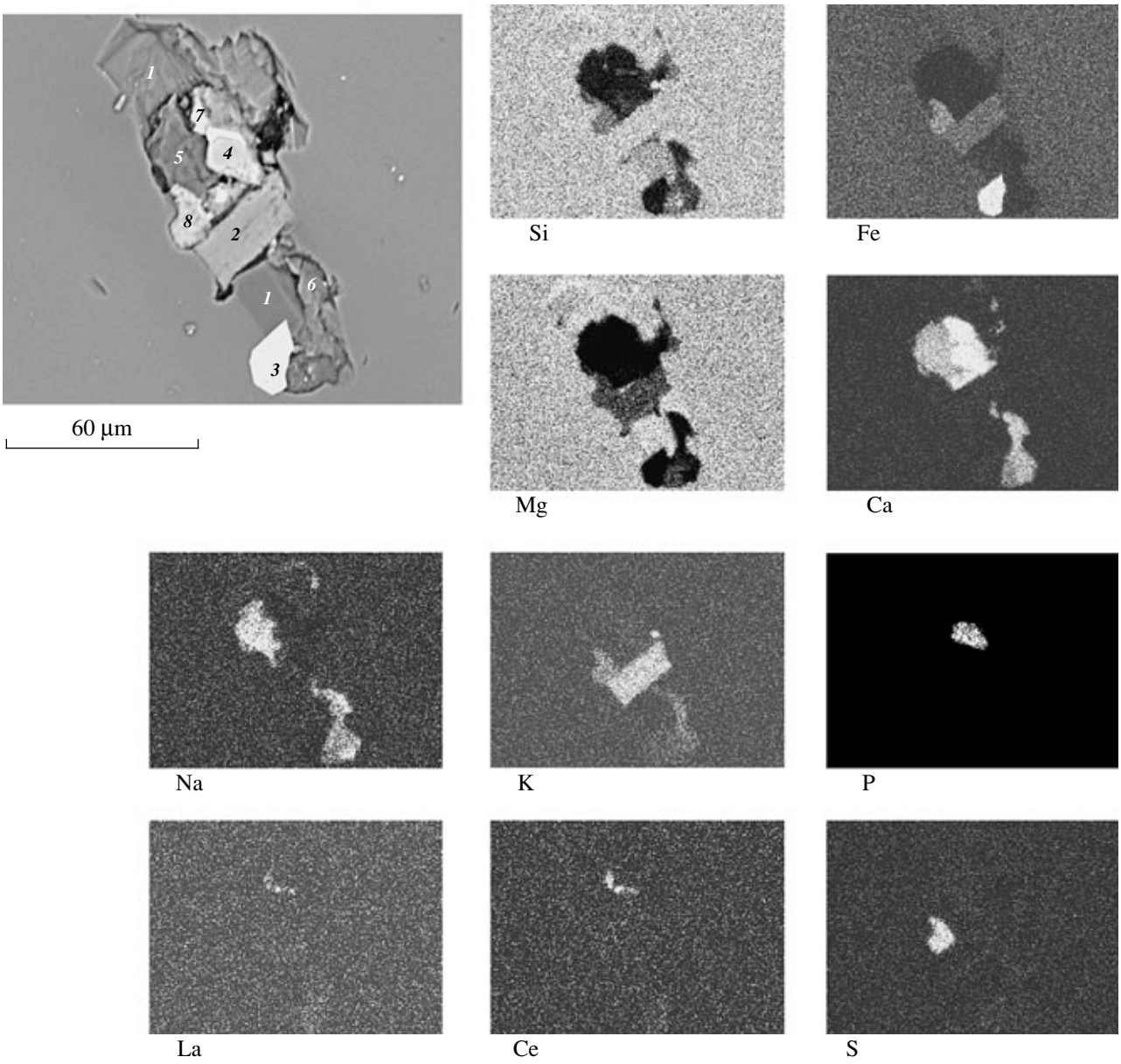

Fig. 4. Back-scattered and characteristic X-ray radiation images of a secondary magmatic inclusion and its daughter phases: (*1*) forsterite, (*2*) tetraferriphlogopite, (*3*) magnetite, (*4*) apatite, (*5*) Na–Ca carbonate, (*6*) K–Na–Ca carbonate, (*7*) Burbankite, (*8*) djerfisherite.

burbankite $(Na,Ca)_3(Sr,Ca,Ba,REE)_3(CO_3)_5$, and a mineral provisionally identified as carbocernaite $(Na,Ca)(Sr,Ba,REE)(CO_3)_2$.

According to the quantitative proportions of their daughter phases, the secondary inclusions are subdivided into two types: one of them is characterized by the predominance of silicates, and the other is dominated by carbonates and ubiquitously bears tetraferriphlogopite and magnetite. Inclusions of each variety are usually spatially separated and restricted to different microfractures, whose intersections suggest that the carbonate inclusions are younger. It should be noted that secondary inclusions having different compositions are known to occasionally occur together.

The secondary inclusions differ from the primary ones not only in their mineral composition, but their analogous daughter phases also have different chemical compositions. The latter are richer in Fe when contained in forsterite; in Sr, Ba, and K when in tetraferriphlogopite; in REE_{Ce} when in apatite and Na–Ca carbonates, and also in Mg when in these carbonates (Tables 3–5). The magnetite of the secondary inclusions is depleted in typical trace elements (Ti, Cr, and Ni), and the Al_2O_3 content in tetraferriphlogopite becomes very low.

CONCLUSIONS

Our data on the composition of crystalline inclusions and daughter minerals of melt inclusions (Tables 2–5) provide insight into the characteristics of the chemical composition and evolution of the melt from which chrysolite crystallized. Evidently, this melt was undersaturated with respect to SiO_2, but enriched in alkalis, CaO, and CO_2. The persistent presence of forsterite (or serpentine), tetraferriphlogopite, clinohumite, and carbonates with elevated Mg concentrations among the daughter phases of the melt inclusions testifies to the high-Mg environment of chrysolite crystallization. The parental melt of the chrysolite was depleted in Al_2O_3, which resulted in the crystallization of tetraferriphlogopite, whose distinctive compositional feature is its relatively low Al_2O_3 concentration [11]. Our data indicate that the average Al_2O_3 concentration in the tetraferriphlogopite included in the chrysolite is 0.68% and decreases to 0.10–0.04% in the daughter phases (Tables 2–4). The melt was poor in F, which was detected only in the earliest apatite-I and was not found in the other minerals potentially able to concentrate this element (the younger apatite, tetraferriphlogopites, amphibole, and clinohumite, which can occur both as younger phases captured by the inclusions and as their daughter phases).

The evolution of the melt controlled by crystallization differentiation at decreasing temperature resulted in the enrichment of salt (carbonate) component and the replacement of Ca-bearing phases (diopside, calcite, and Na–Ca carbonates in the primary inclusions) by Mg-bearing minerals (dolomite, Na–Ca carbonates, and Na–Mg carbonates in the secondary inclusions). As follows from the composition of the secondary inclusions, the residual melts that were enriched in carbonate components concentrated trace elements and REE in the form of Sr-bearing barytocalcite and Ba–Sr–REE carbonates. Simultaneously, S and Cl were accumulated in djerfisherite, Cl in northupite, and Fe in daughter forsterite (which contains 7.4 mol % of the fayalite end member, whereas the forsterite phase of the primary inclusions contains 4.9 mol % fayalite). The accumulation of K resulted in the occurrence of djerfisherite and K–Na–Ca carbonate among the daughter phases. Many of the daughter phases of the chrysolite-hosted inclusions from the phlogopite deposit (first of all, calcite, dolomite, Na–Ca, and Na–Mg carbonates) were found in the melt inclusions of forsterite from the phoscorites and carbonatites of the Kovdor apatite–magnetite deposit [15, 16]. This suggests genetic relations between the rocks composing these deposits. However, geological and petrological data contradict this assumption. The formation of the phoscorite–carbonatite association in this massif was supposedly related to the differentiation of alkaline melanephelinite melts [15], whereas the rocks of the phlogopite deposit are considered to be unusual ultrabasic pegmatites [7].

The discovery of melt inclusions (in the complete absence of fluid inclusions) in the chrysolite is at variance with its supposedly hydrothermal–metasomatic nature [17]. The presence of melt inclusions in forsterite from all varieties of the phlogopite-bearing rocks ([12] and our unpublished data) testifies, first of all, to a magmatic genesis of the Kovdor phlogopite deposit and, second, to the affiliation of the chrysolite occurrence in this massif with the magmatic genetic class.

The recrystallized multiphase inclusions of a carbonate–silicate composition with an unusual assemblage of daughter phases have never been found in chrysolite from deposits of other genetic types [1, 4]. A combination of these melt inclusions with crystalline inclusions of apatite, tetraferriphlogopite, amphibole, and magnetite can be regarded as an additional identification feature of gem-quality chrysolite from the Kovdor Massif.

REFERENCES

1. E. Ya. Kievlenko, *Geology of Gems* (Zemlya, Moscow, 2001) [in Russian].
2. E. J. Gübelin and J. I. Koivula, *Photoatlas of Inclusions in Gemstones* (ABC Edition, Zurich, 1992).
3. P. Maaskant, "Electron Probe Microanalysis of Unopened Fluid Inclusions, a Semiquantitative Approach," Neues Jahrb. Mineral., Monatsh., No. 7, 297–304 (1986).
4. S. V. Sokolov, S. A. Yarmishko, and A. V. Fedorov, "Gem-Quality Chrysolite with New Types of Inclusions," Vestn. Gem., No. 6, 49–54 (2002).
5. A. A. Kukharenko, M. P. Orlova, A. G. Bulakh, et al., *Caledonian Complex of Ultramafic Alkaline Rocks and Carbonatites in the Kola Peninsula and Northern Karelia* (Nedra, Moscow, 1965) [in Russian].
6. V. I. Ternovoi, B. V. Afanas'ev, and B. I. Sulimov, *Geology and Exploration of the Kovdor Vermiculite–Phlogopite Deposit* (Nedra, Leningrad, 1969) [in Russian].
7. N. I. Krasnova, "The Kovdor Phlogopite Deposit, Kola Peninsula, Russia," Can. Mineral. **39**, 33–44 (2001).
8. S. A. Yarmishko, S. V. Sokolov, and V. A. Rassulov, "Spectroscopic Properties of the Kovdor Chrysolite," *Proceedings of 6th International Conference on New Ideas in the Earth Sciences, Moscow, Russia, 2003* (Moscow, 2003), Vol. 2, p. 131 [in Russian].
9. S. V. Sokolov and N. V. Chukanov, "Carbon-Bearing Compounds in Inclusions from the Minerals in the Kovdor Massif (Kola Peninsula, Russia)," Acta Mineral.-Petrograph. Abstract Ser., No. 2, 192–193 (2003).
10. A. N. Platonov, M. N. Taran, A. D. Khar'kiv, et al., "Study of Features of the Colors of the Gem-Quality Chrysolite," in *Constitution and Properties of Minerals* (Naukova Dumka, Kiev, 1977), No. 11, pp. 41–49 [in Russian].
11. O. M. Rimskaya-Korsakova and E. P. Sokolova, "On Ferruginous–Magnesian Micas with Reverse Absorption," Zap. Vses. Mineral. O-va, No. 4, 411–423 (1964).
12. N. I. Krasnova, Yu. A. Mikhailova, T. Villiams, and Yu. L. Kretser, "Inclusions in Olivine from Rocks of the Kovdor Alkaline–Ultramafic Complex as Indicators of

the Compositional Evolution of the Mineral Formation Environment," in *Synthesis of Minerals and Methods of Their Investigations*, Tr. VNIISIMSa **16**, 259–265 (2000).

13. T. A. Smirnova, "Exsolution Lamellae in Olivine from Ultramafic Rocks," Zap. Vses. Mineral. O-va, No. 2, 209–212 (1971).
14. A. F. Cooper, J. Gittins, and O. F. Tuttle, "The System Na_2CO_3–K_2CO_3–$NaCO_3$ at 1 kbar and Its Significance in Carbonatite Petrogenesis," Am. J. Sci. **275**, 534–560 (1975).
15. I. V. Veksler, T. F. D. Nielsen, and S. V. Sokolov, "Mineralogy of Crystallized Melt Inclusions from Gardiner and Kovdor Ultramafic Alkaline Complexes: Implications for Carbonatite Genesis," J. Petrol. **39**, 2015–2031 (1998).
16. S. V. Sokolov, "Carbonate Daughter Phases of Melt Inclusions in the Minerals from Rocks of Carbonatite Complexes," in *Synthesis of Minerals and Methods of their Investigations*, Tr. VNIISIMSa **16**, 282–294 (2000).
17. Yu. N. Tarasenko, M. A. Litsarev, L. I. Tret'yakova, and A. Ya. Vokhmentsev, "Chrysolite from the Kovdor Phlogopite Deposit," Izv. AN SSSR. Seriya Geol., No. 9, 67–80 (1986).